Benzylation of Arenes with Benzyl Chloride over H-Beta Zeolite: Effects from Acidity and Shape-selectivity

Zichun Wang,[a] Lei Wang,[b] Zheng Zhou,[a] Yunyao Zhang,[a] Haitao Li,[a] Catherine Stampfl,[c] Changhai Liang[b] and Jun Huang[a]**

[a] Laboratory for Catalysis Engineering, School of Chemical and Biomolecular Engineering, The University of Sydney, NSW 2006, Australia

[b] Laboratory of Advanced Materials and Catalytic Engineering, School of Chemical Engineering, Dalian University of Technology, Dalian 116024, China

[c] School of Physics, The University of Sydney, NSW 2006, Australia

ABSTRACT H-Beta zeolites with various Si/Al ratios have been prepared for the liquid-phase benzylation of various arenes with benzyl chloride (BzCl). ^{29}Si and ^{27}Al MAS NMR spectroscopy revealed the incorporation of Al into the silica framework to form catalytically active Brønsted acid sites (BAS). ^{1}H MAS NMR spectroscopy investigations demonstrated the BAS density increased with reducing Si/Al ratio, while the BAS strength slightly decreased as probed by CD_3CN molecules. These H-Beta zeolites are highly selective to desired monobenzylation products depending on the shape-selectivity induced by the suitable channel system. The catalytic performance is in line with the nucleophilicity and proton affinity (PA) of arenes (xylene > toluene > benzene) on the same catalyst, typically for Friedel-Crafts reaction. A shape-selective effect has been observed to dominate the reaction, lowering the performance of mesitylene compared to xylene, as well as being selective to only the monobenzylation product. The benzylation performance is significantly enhanced with increasing both the BAS density and strength of H-Beta zeolites due to the formation of more aryl cation intermediates by attacking electronegative chlorine atom in BzCl. An alternative reaction mechanism based on the activation of arenes by protonating aromatic ring of BAS is proposed to explain the superior benzylation activity of BzCl with less active arenes.

KEYWORDS Beta zeolite; Benzylation reaction; shape selectivity; surface sites; solid-state NMR spectroscopy.

■ INTRODUCTION

Liquid-phase alkylation of arenes is a typical Friedel-Crafts reaction to produce industrially important compounds, e.g. diphenylmethane (DPM) and its derivates, used in organic chemistry and pharmaceuticals.[1] Benzylation of arenes with benzyl chloride (BzCl) or benzyl alcohol provides a single-step method to synthesize these products, which has attracted great attention industrially.[2] In practice, benzylation reactions are catalyzed by homogeneous metal halides ($AlCl_3$, $FeCl_3$, $InCl_3$, BF_3, etc.) and Brønsted acids (H_2SO_4, HCl, HNO_3, etc.).[3-7] However, these processes are characterized by low selectivity, and inherent problems with requiring stoichiometric catalysts, the toxic and corrosive nature of the catalyst, as well as difficulties in catalyst separation and regeneration.[8,9]

Aiming to overcome these drawbacks, extensive efforts have been devoted to develop green chemical processes for the efficient production of DPM and derivates based on solid acid catalyst. Various zeolites and mesoporous silica-alumina,[2, 10-16] sulfated ZrO_2 and Fe_2O_3,[17,18] heteropoly acids (HPAs),[19] supported metal halides and HPAs [20-23] were all tested. Due to the free diffusion of benzylation reagent on metal oxides, metal halides and HPAs often contribute higher conversion, but less selectivity to the desired monobenzylation product.[2, 20] Microporous zeolite-based catalysts providing shape-selectivity are promising for preventing the secondary reactions that generate undesired polyalkylated byproducts by using homogeneous catalysts and other solid acids,[13, 19-20] which also have excellent stability, relatively low costs, commercial availability, and widespread in-depth knowledge of zeolite-mediated reactions.[24-26]

Commonly used zeolites (H-ZSM-5, H-Y, and Hβ) have been investigated in benzylation reactions.[11, 27] The H-ZSM-5 zeolite showed nearly no activity (e.g. BzCl conversion of 2.8 %) for the benzylation of benzene due to diffusion limitation inside channel systems.[11, 13] The H-Y

zeolite yields the highest BzCl conversion (64.1 %), but the large pore size and inner cavity (from 7.4 to 12 Å)[28] allow the production of undesired polyalkylated products with the highest selectivity of 35.2 %, in comparison with the zeolites H-ZSM-5 and Hβ under the same conditions.[11] The Hβ zeolite, possessing a 12-membered ring apertures of 5.6-7.3 Å,[29] provides a better diffusion of arenes and is considerably more shape-selective to the desired monobenzylation product.[13, 15]

The active sites in zeolites, Brønsted acid sites (BAS), are generated by a proton compensating the negatively charged oxygen atom after Al^{3+} replacing framework Si^{4+}.[25] Previous work reported increasing the Si/Al ratio of Hβ zeolites from 52 to 160 lead to a higher BzCl conversion.[15] Often, incorporating more Al atoms into the framework can enhance the density of BAS on the Hβ zeolites, but reduce the overall acid strength of BAS due to the decrease of the mean electronegativity of the framework.[30-31] But the detailed investigation of the acidity effect (density and strength) with the nucleophilicity and molecular size of arenes on the benzylation reaction over Hβ zeolite is urgent to fill the gap between zeolite structure and catalytic performance.

In this work, we performed a systematic study to investigate the relationship between the physical/chemical properties of the Hβ zeolite and the benzylation of arenes (various nucleophilicity and size) with BzCl. Hβ zeolites with various Si/Al ratios between 10 and 30 have been prepared by hydrothermal technique. A detailed study on BAS density and strength of these catalysts was investigated by ^{1}H MAS NMR spectroscopy. All the prepared Hβ zeolite catalysts are active and highly selective to the monobenzylation products in the benzylation of arenes with BzCl. Whereas, the benzylation product distribution is independent on the acidic properties of the Hβ zeolite. The BAS density and strength of zeolites mainly govern the catalyst

activity in benzylation reactions in the selected temperature range. Since the BzCl conversion is beyond the control of nucleophilicity of arenes, a new reaction mechanism has been proposed.

■ EXPERIMENTAL

Catalyst Preparation. All chemicals used for the preparation of Beta zeolites, such as silica sol (40.0 % SiO_2, Akzo Nobel), tetraethyl ammonium hydroxide aqueous solution (25.0 % TEAOH, Tianjin Guangfu Fine Chemical Research Institute), sodium aluminate (43.5 % Al_2O_3, 46.5 % Na_2O, Sinopharm Chemical Reagent Co., Ltd.), sodium hydroxide (99.0 % NaOH, Sinopharm Chemical Reagent Co., Ltd), were purchased. For the preparation of beta zeolites, sodium aluminate was firstly dissolved in TEAOH aqueous solution, followed by mixing with NaOH aqueous solution and silica sol under vigorous stirring. Then, 500 mL of the final gel mixture, having a molar composition of SiO_2:Al_2O_3:Na_2O:$(TEA)_2O$:H_2O = 62:*x*:5.1:12.5:1300, was transferred into a 1.0 L stainless-steel autoclave, where *x* was adjusted based on requirement. The crystallization process was conducted at 413 K for 4 days with a stirring speed of 40 rpm. Then, the solid products were separated by centrifugation and dried at 353 K for 12 h, followed by calcination at 823 K for 2 h under an air atmosphere to remove organic templates.

Ammonia exchange with the obtained Naβ zeolites was employed to prepare Hβ zeolites as described in our earlier work.[32] Briefly, Naβ zeolite was mixed with certain amount of 0.1 M NH_4NO_3 aqueous solution and stirred at 353 K for 3 h. After filtration and wash with deionized water till no nitrate ions can be detected, the obtained product was dried at room temperature overnight. The above procedure was repeated for four time to ensure ion-exchange degree > 99 % in the final Hβ zeolites. All obtained Beta zeolites were dissolved in HF solution and analyzed by atomic emission spectroscopy with an inductively coupled plasma (ICP-AES, Perkin–Elmer,

Plasma 400). The results of the chemical analysis are listed in Table 1. The nomenclature of Beta zeolites is defined as Hβ*x*, where *x* is assigned to 1-4.

BET measurements. Nitrogen adsorption-desorption measurements were performed by an Autosorb IQ-C system to determine the specific surface areas. Before measurements, the zeolite samples were degassed at 423 K under vacuum to remove adsorbates from the surface. The specific surface areas were determined by BET measurement and are summarized in Table 1.

X-ray characterization (XRD). The XRD patterns of Beta zeolites were recorded on a Rigaku D/Max-RB diffractometer with a Cu-Kα monochromatized radiation source (λ = 0.154 nm, 40 kV, 100 mA).

Solid-state NMR. For ^{27}Al and ^{29}Si MAS NMR investigation, all samples were exposed to the saturated vapor of $Ca(NO_3)_2$ solution at ambient temperature overnight in a desiccator for fully hydration. For ^{1}H MAS NMR experiments, the samples were dehydrated at 723 K under a N_2 flow rate of 50 mL. These dehydrated samples were also subjected for *in situ* loading with acetonitrile-d_3 at room temperature and purged under a N_2 flow rate of 50 mL for 10 min to remove weakly physisorbed molecules. Subsequently, the samples were transferred into the MAS NMR rotors under dry nitrogen gas inside a glove box.

^{1}H and ^{27}Al MAS NMR investigations were carried out on an Agilent DD2-500 MHz spectrometer at resonance frequencies of 400.1 and 104.3 MHz with the sample spinning at the rate of 8 kHz using 4 mm MAS rotors. Spectra were recorded after single-pulse π/2 and π/6 excitation with repetition times of 20 s and 1 s for studying ^{1}H and ^{27}Al nuclei, respectively. Quantitative ^{1}H MAS NMR measurements were performed using the H,Na-Y zeolite (35 % ion-exchanged) as an external intensity standard, which contains 58.5 mg zeolite H,Na-Y with 1.776 mmol OH/g. ^{29}Si MAS NMR experiments were performed on the same spectrometer at the

resonance frequency of 79.5 MHz and with the sample spinning rate of 4 kHz using a 7 mm MAS rotor. For ^{29}Si MAS NMR, single-pulse π/2 excitation and high-power proton decoupling with a recycle delay of 20 s was applied. To separate the different signals and for the quantitative evaluation of spectra, the data were processed using the Bruker software WINNMR and WINFIT.

Benzylation of Arenes with Benzyl Chloride. Prior to reaction, 3.50 mL arene (benzene, toluene, xylene or mesitylene) and 0.25 mL benzyl chloride (Arene/BzCl molar ratio was 14:1) were mixed and added into a three-necked-round bottom flask equipped with a reflux condenser, nitrogen gas tube, and needle for reactant injection and sample collecting. Then the mixture was kept at reaction temperature for 10 min under stirring and N_2 flow. Subsequently, the activated catalyst (25 mg) was added into flask, and this time is regarded as initial reaction time. The employed catalyst was pretreated in a tube reactor under a N_2 flow of 50 mL/min at 723 K overnight, followed by cooling down to room temperature under flowing N_2 gas. Samples of benzylation products (30 μL) were collected periodically and dissolved in ethanol solvent (1.00 ml) for analysis. The reaction products were analyzed using a Shimadzu GCMS-QP2010 Ultra equipped with a Rtx-5MS capillary column (30 m × 0.25 mm × 0.25 □m) connected with a mass spectrometer for qualitative analysis, as well as a RTX-5 capillary column (30 m × 0.32 mm × 3 μm) connected with a GC-FID detector for quantitative analysis. Conversion, selectivity and yield were calculated by:

$$Conversion\ \% = \frac{A_{p1}+A_{p2}}{A_{p1}+A_{p2}+A_r} \times 100\ ;\ Selectivity\ \% = \frac{A_{p1}\ or\ A_{p2}}{A_{p1}+A_{p2}} \times 100\ ;.$$

where A_{p1} and A_{p2} were the peak areas of benzylation products in the GC analysis, A_r was the peak area of BzCl.

■ RESULTS AND DISCUSSION

Physical characterization of Hβ Zeolite. The structure of the obtained Hβ zeolites was confirmed by X-ray diffraction (XRD) and the corresponding patterns are shown in Fig. 1. All samples displayed three main diffraction peaks at 2θ = 7.7°, 22.3° with a shoulder of 21.3° and 43.5° corresponding to (110), (302) and (220) planes, respectively. It indicates a typical BEA topology pattern of beta-zeolite,[33] and no obvious diffraction signal of crystalline Al species can be detected.

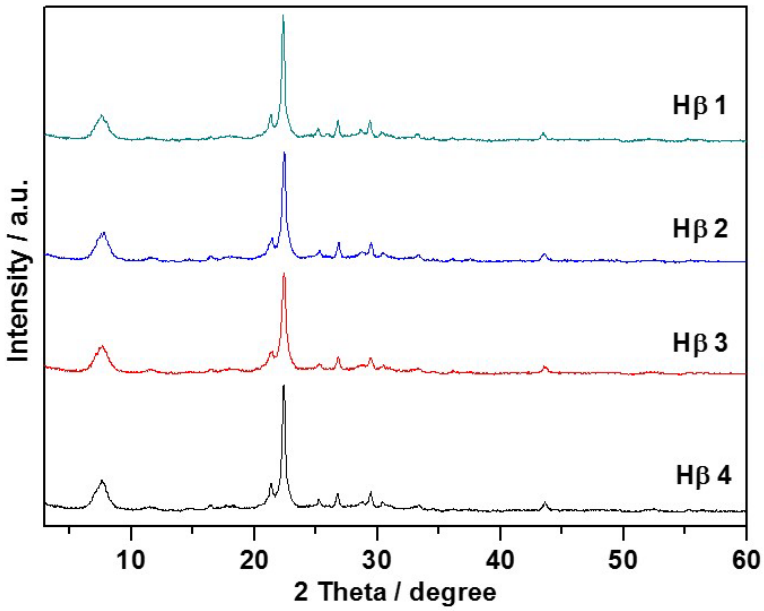

Figure 1. XRD patterns of Hβ1 (green), Hβ2 (blue), Hβ3 (red), and Hβ4 (black).

Table 1. Structural Data and Chemical Composition of Hβ Zeolites

Beta	Hβ1	Hβ2	Hβ3	Hβ4
Specific surface areas[a] (m^2/g)	517	539	556	543
Average pore size[a] (nm)	1.36	1.37	1.39	1.31
Total pore volume[a] (cm^3/g)	0.352	0.362	0.387	0.356

Si/Al ratio (ICP)[b]	10.8	14.2	29.0	30.4
BAS density (mmol/g)[c]	0.52	0.45	0.43	0.41
BAS strength ($\Delta\delta_{1H}$ / ppm) [d]	7.1	7.3	7.4	7.5
Number of BAS (per nm^2)[e]	0.61	0.50	0.47	0.45

[a] Determined by nitrogen adsorption-desorption isotherms. [b] Si/Al ratios determined by ICP analysis. [c] The density of Brønsted acid sites (BAS) were determined by the corresponding ^{1}H MAS NMR spectra. [d] Determined by ^{1}H MAS NMR spectra of dehydrated Hβ loaded with CD_3CN shown in Fig. 5. [e] Calculated by (BAS density×Avogadro constant)/specific surface area.

The specific surface areas of Hβ zeolites with different Si/Al ratios were obtained by N_2 adsorption-desorption isotherms and are summarized in Table 1. All Hβ zeolites exhibit similar specific surface area (517-556 m^2/g) and total pore volume (0.35-0.38 cm^3/g) in the range for typical Beta zeolites.

Local structure in zeolite Hβ measured by ^{27}Al, ^{29}Si and ^{1}H NMR. The acidity and local structure properties of the obtained Hβ zeolites were investigated by solid-state NMR spectroscopy. As shown in Fig. 2, the strong signals at δ_{27Al} = 54 ppm assigned to Al^{IV} species indicates most of Al atoms were incorporated into the silica framework of the Beta zeolites, while a small amount of extra-framework Al species (EFAl) increased with decreasing Si/Al ratio indicated by increasing the signal intensity of octahedral Al (Al^{VI}) at 0 ppm. In general, the BAS in zeolites are generated by protons compensating the negative charges that are generated by the substitution of Si atoms in zeolite framework by Al atoms showing tetrahedral coordination (Al^{IV} species).[32, 34-36] EFAl (generally considered as Lewis acid sites (LAS)) inside zeolite pore channels,[25] increasing in the order of Hβ1 (0.08 mmol/g) > Hβ2 (0.06 mmol/g) > Hβ4 (0.03 mmol/g) > Hβ3 (0.02 mmol/g).

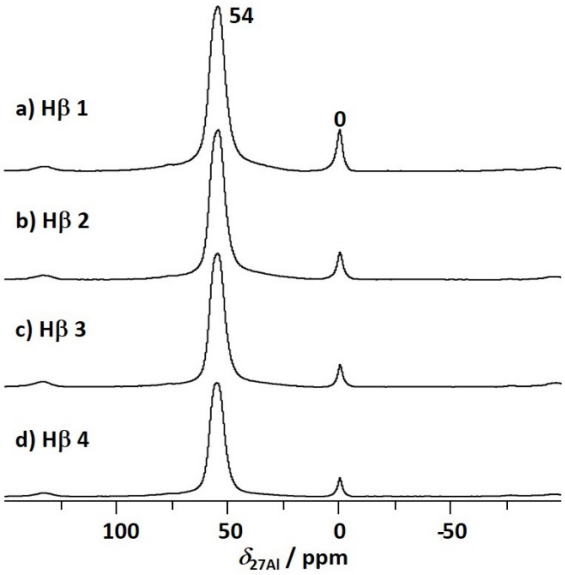

Figure 2. ^{27}Al MAS NMR spectra of Hβ zeolites.

The incorporation of Al atoms into the silica framework has also been confirmed by the formation of Si(1Al) species as shown in the simulation result of the corresponding ^{29}Si MAS NMR spectrum (Fig. 3). The Si(0Al) and Si(1Al) species indicates 0 or 1 Al atom is incorporated in the second coordination of Si atom at the T-position, e.g. $Si(OSi)_3OAl$, while the Q^3 species was assigned to terminal hydroxyl groups bounded to Si atoms as $Si(OSi)_3OH$ species. The concentration of Si(1Al) gradually increased with reducing Si/Al ratios from Hβ1 to Hβ4. Increasing framework Al species can promote the formation of surface BAS by a proton compensation. These BAS are key active sites for benzylation of arene with BzCl over zeolites.[11, 27] Quantifying the density and strength of surface BAS is of great importance for understanding structure-performance relationships.

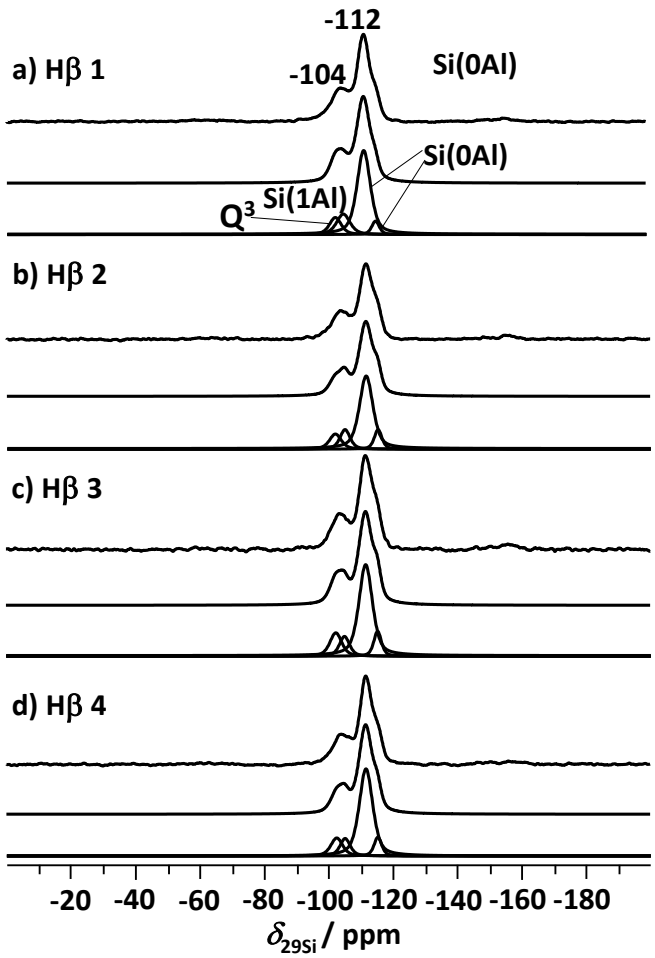

Figure 3. ^{29}Si MAS NMR spectra of Hβ zeolite.

Quantitative evaluation of BAS can be achieved with simulating the ^{1}H MAS NMR spectra of dehydrated beta zeolites, since the ^{1}H low-field chemical shift of BAS can be clearly distinguished from other hydroxyl groups on zeolites. The simulation results of ^{1}H MAS NMR spectra (Fig. 4 bottom) shows a strong signal at ca. 1.8 ppmdue to terminal SiOH groups, while two weak signals at ca. 0.7 and 2.2 ppm are caused by AlOH groups (from EFAl species) bounded to neighboring OH groups.[37] The strong low-field signal at ca. 4.1 ppm with a broad hump at 5.2 ppm were assigned to bridging SiOHAl groups and disturbed bridging SiOHAl groups, respectively.[38-40] The densities of BAS are evaluated by the signals of bridging OH

groups (δ_{1H} = 4.1-5.2 ppm). As summarized in Table 2, the density of BAS increased from 0.41 mmol/g to 0.52 mmol/g with decreasing Si/Al ratios from 30.4 to 10.8. It indicates that more and more Al atoms were incorporated into the silica framework to contribute to surface BAS.

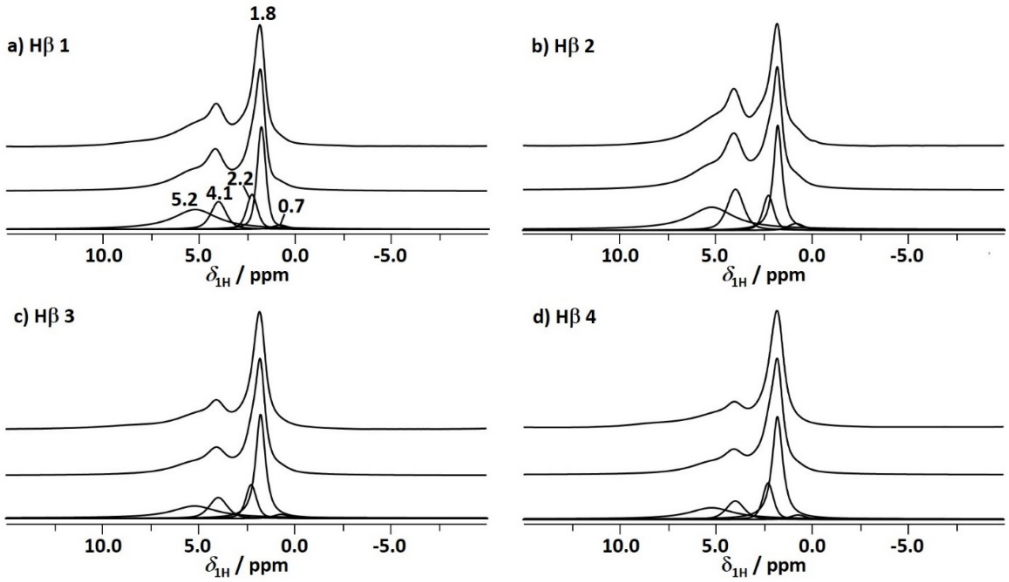

Figure 4. ^{1}H MAS NMR spectra of the dehydrated (723 K) zeolites Hβ1 (a), Hβ2 (b), Hβ3 (c) and Hβ4 (d) and their simulations (bottom).

Increasing the framework Si/Al ratio or the presence of EFAl species can enhance the acid strength of bridging hydroxyl protons.[41-43] The acid strength of various surface OH groups are often scaled by their ^{1}H low-field shift ($\Delta\delta_{1H}$) induced upon acetonitrile-d_3 (CD_3CN) adsorption.[25, 32] CD_3CN hydrogen-bounded to SiOH groups (SiO–H···N) shifted the main SiOH signal (δ_{1H} = 1.8 ppm) to low field ($\Delta\delta_{1H}$ = 3.3 ppm) as shown in Fig. 5, typically for weakly acidic SiOH groups. The $\Delta\delta_{1H}$ value ($\Delta\delta_{1H}$ = 7.1 ppm) for bridging OH groups on the zeolite Hβ1 is over two times larger than weakly acidic SiOH groups, in line with their instinct strong BAS acidity. Two kinds of bridging OH groups were identified in the ^{1}H MAS NMR spectra of Hβ zeolites (Fig. 4), which are characterized with the similar acid strength according to

literature.[44,45] The ^{1}H MAS NMR of acetonitrile-d_3 loaded samples exhibit the similar mobility on all Hβ zeolite but the low-field shift of the signal centers correlates the increase of acid strength. Hβ1 and Hβ2 exhibit the similar acid strength with the similar signal centers, which is slightly lower than that on Hβ3 and Hβ4 due to the slightly low-field shift of the signal centers.

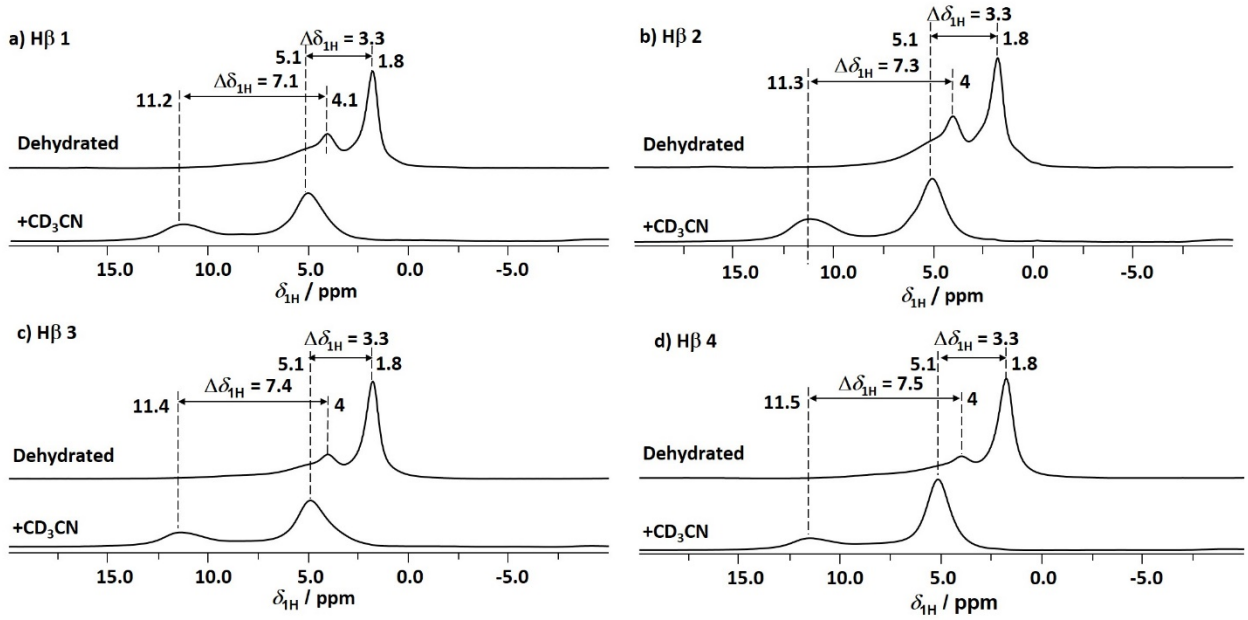

Figure 5. ^{1}H MAS NMR spectra of dehydrated Hβ with different Si/Al ratio of Hβ1 to Hβ4, recorded before (top) and after (bottom) adsorption of CD_3CN at room temperature and purged with under a N_2 flow of 50 mL for 10 min.

Benzylation of Arenes with Benzyl Chloride. The obtained Hβ zeolites were utilized for the benzylation of arenes (benzene, toluene, xylene, or mesitylene) with benzyl chloride as shown in Scheme 1.

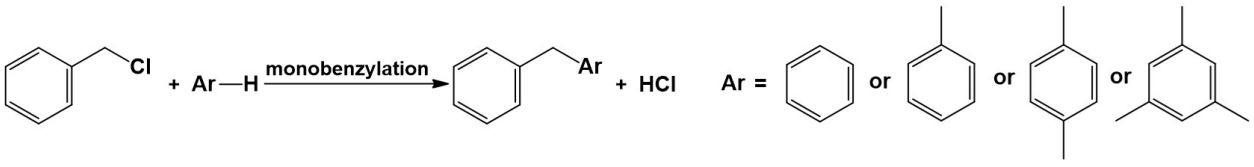

Scheme 1. Benzylation of BzCl with different arenes**.**

As an example, Fig. 6 displayed the benzylation of different arenes with BzCl over Hβ3 (as the best catalyst in the current study). It shows that the conversions of BzCl with all arenes were increased as a function of reaction time. The reaction rate *k* increased in the order of xylene > toluene > benzene (Table. 2), which is typical for Friedel-Crafts reactions since the increase of nucleophilicity and proton affinity (PA) of arenes can facilitate the electrophilic substitution on aromatic rings.[1] This is opposite to that reported previously (benzene > toluene > xylene > mesitylene) over mesoporous [Al]SBA-15 (Si/Al = 45), which was attributed to a stronger adsorption of arenes on active sites with a higher nucleophilicity.[12] However, this phenomenon was not observed with our Hβ zeolites, which normally exhibits much higher acidity than amorphous [Al]SBA-15.

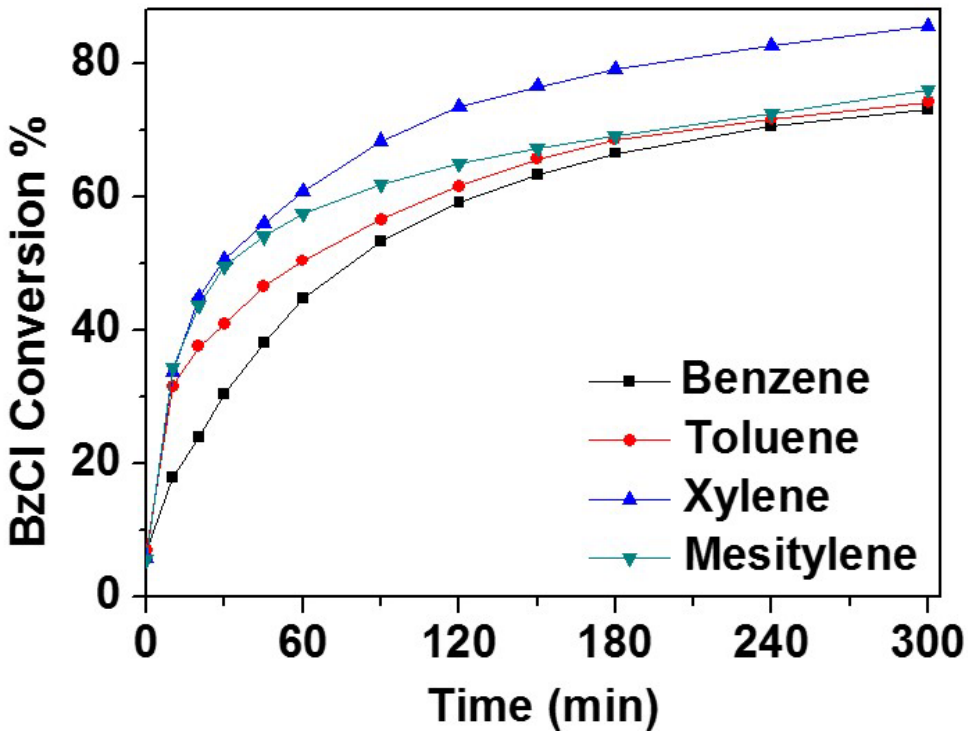

Figure 6. Benzylation of benzyl chloride with different arenes at 353 K over Hβ3.

Table 2. Nucleophilicity and PA values for arenes, and rate constant *k* obtained over the Hβ3 zeolite.

			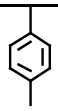	
Nucleophilicity[a]	-4.38	-3.94	-3.39	-2.82
PA Value (kJ/mol)	750.2	784.1	794.5	836.4
k at 353 K (10^{-4} min^{-1})[b]	41.4	63	93	69

[a] Nucleophilicity parameter was acquired from Mayr's equation, log*k*=S(N+E), in which E (Electrophilicity parameter) of An_2CH^+ was defined as 0 and S (nucleophile-specific Slope parameter) of 2-methyl-1-pentene was defined as 1. [b] Since the concentration (C_{arenes}) ≫ C_{BzCl}, *k* was determined by $-\ln(1-X_{BzCl})=kt$, where X_{BzCl} is BzCl conversion and *t* is reaction time (min) obtained from Fig. 6.

Notably, mesitylene with higher nucleophilicity and PA, yielded an obviously lower BzCl conversion (75.9 % and 1.15×10^{-4} s^{-1}) than xylene (85.6 % and 1.55×10^{-4} s^{-1}). Here, the pore size of Hβ is comparable to the molecular size of arenes (ca. 0.67-0.80 nm).[46] The large molecular size of mesitylene (0.80 nm) strongly affects the mass transfer of mesitylene molecules, bimolecular reaction, and product diffusion inside pores and channels in comparison with xylene due to the shape selectivity of zeolites,[47] affording a 26 % decrease of *k* (Table 2). The shape-selective effect has also been observed to strongly influence the product distribution. As shown in Table 3, a 100 % selectivity to desired monobenzylation products is yielded in the benzylation of all arenes with a large consumption of BzCl. This is benefited from the suitable pore size and channel system of Hβ zeolites to prevent the further alkylation of monobenzylation product (molecular size estimated from 0.7 to 1.0 nm) to form polyalkylated byproduct with larger molecular size. Two monobenzylation products were obtained with toluene over the studied Hβ zeolites, with a selectivity of 1-benzyl-4-methylbenzene (4-BMB, 89.7-91.2 %) and a

selectivity of 1-benzyl-2-methylbenzene (2-BMB, 8.8-10.3 %). This is attributed to the addition of benzyl cation on the ortho-position of toluene (2-BMB) suffers from a stronger steric hindrance than that on para-position (4-BMB). The absence of meta-adduct was also observed, since the electro density of the mata-position (0) is lower than that of the ortho- & para-position (-0.017 & -0.01, respectively), resulting in a poor nucleophilicity towards benzyl cations.

Benzylation of arenes with BzCl is a typical acid-catalyzed reaction. It has been reported previously that catalysts with mainly Lewis acidity,[48-49] such as Ga–Mg-hydrotalcite, are not active for benzylation of arenes with benzyl chloride. Therefore, the acidity investigations are focus on identifying the effect of the density and strength of BAS. The conversion of BzCl in arenes over Hβ zeolites has been performed as a function of time shown in Fig. 7 and the results are summarized in Table 3. Clearly, the BzCl conversion with toluene significantly enhanced from 59.6 to 99.3 % (Fig. 7a and Table 4 entry 2). Hβ3 and Hβ4 having lower BAS density and slightly higher strength than those on Hβ1 and Hβ2 exhibit a significantly higher catalytic performance. With similar BAS strength, Hβ1 having a higher BAS density achieved a lower performance than Hβ2, while Hβ3 with a higher BAS density obtained a higher performance than Hβ4. A similar trend was also observed with xylene, but benzylation of mesitylene over various Hβ zeolites exhibited a similar BzCl conversion from 94.0 to 98.2 %.

Table 3. Selectivity and Yield in the benzylation of Arenes with BzCl.[a]

Arenes	Products	Selectivity%	Yield %			
			Hβ1	Hβ2	Hβ3	Hβ4
	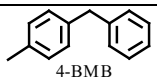 4-BMB	89.7 ~ 91.2	57.8	89.9	90.7	91.1

	2-BMB	8.8 ~ 10.3	6.6	8.8	9.3	8.9
	BDB	100	88.5	99.9	100	100
	BTB	100	95.1	98.1	98.3	98.0

[a] Conditions: 25 mg Hβ, 3.5 ml arenes (benzene, toluene, xylene or mesitylene) with 0.25 ml benzyl chloride, reaction was carried out at 383 K for 240 min.

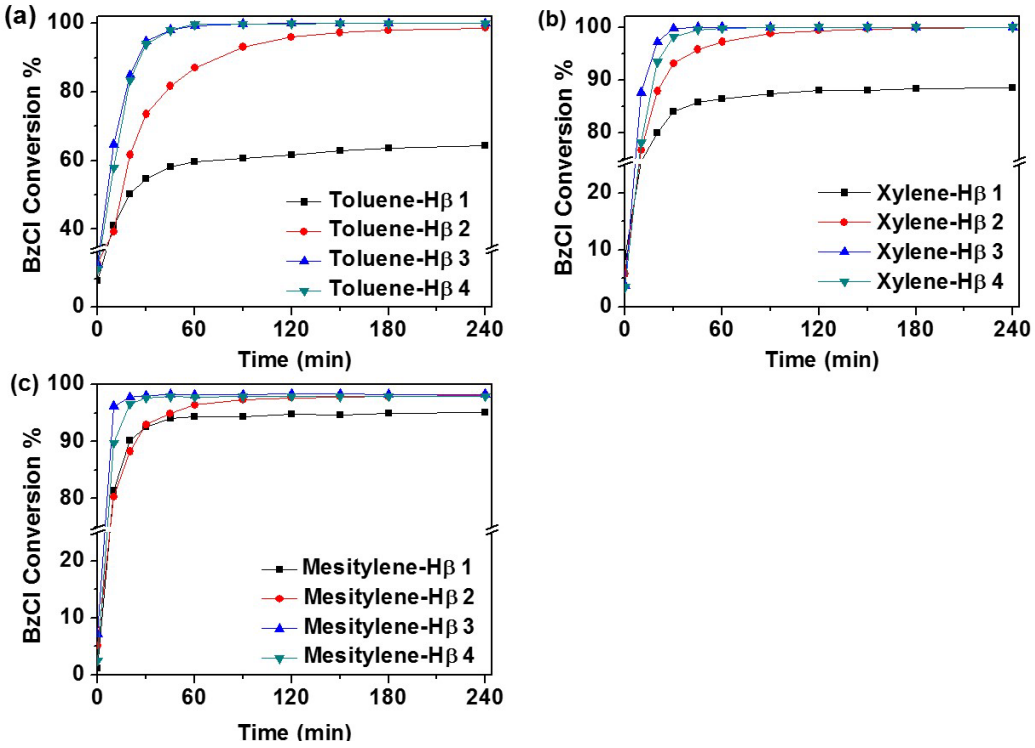

Figure 7. Conversion of BzCl in benzylation of BzCl with arenes over Beta zeolites under the conditions shown in Table 3.

Table 4. BzCl conversion over Hβ1 to Hβ4 at 383 K for 60 min.[a]

	Hβ1	Hβ2	Hβ3	Hβ4

	59.6	87.0	99.3	98.7
	86.5	97.2	100.0	99.8
	94.0	96.4	98.2	97.8

[a] Conditions: 25 mg Hβ, 3.5 ml arene (toluene, xylene or mesitylene) with 0.25 ml benzyl chloride.

A widely accepted benzylation mechanism (Scheme 2 Route 1) is BzCl can be initiated by the formation of benzyl cations ($C_6H_5CH_2^+$) on surface BAS, which attack the aromatic ring for electrophilic substitution to release a proton and generate the final products. The formation of carbocation intermediates can be promoted on BAS with higher acid strength,[50] or higher BAS density at the similar strength, similar as observed with our Hβ zeolites. The lower BzCl conversion on Hβ1 than Hβ2 has been attributed to more EFAl species on surface, which may affect the diffusion of arenes and derivatives inside zeolites pores and channels through adsorption via the strong electronegativity of aromatic rings as reported for alumina.[51-53]

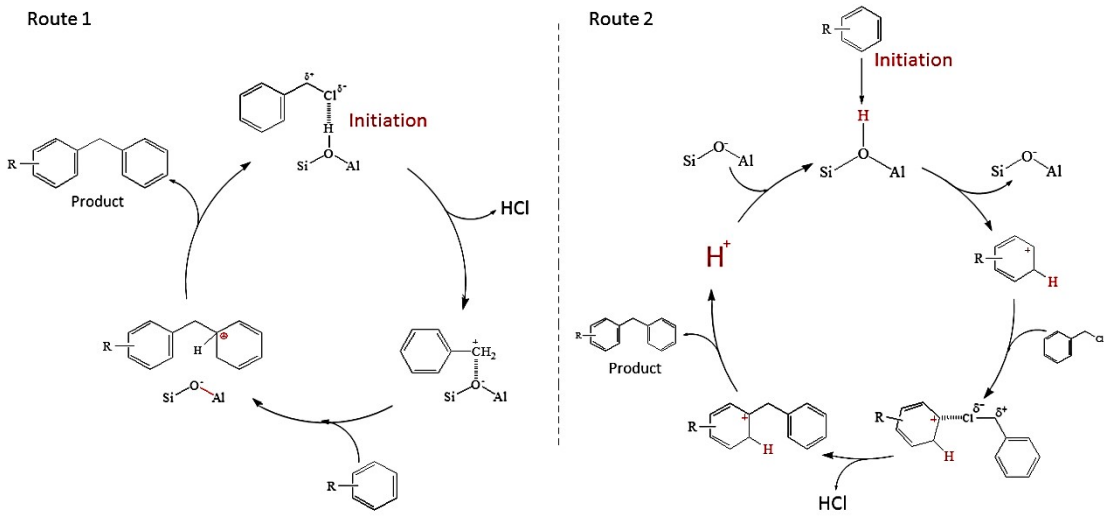

Scheme 2. Proposed benzylation mechanism for BzCl with arenes over BAS on Hβ.

Moreover, alkyl groups as nucleophilic reagents contribute electron donation to aromatic rings, resulting in a higher nucleophilicity and PA of arenes with more substituted methyl groups (Table 2). It can facilitate the attack of the aromatic ring by benzyl cations.[1] The activation of arenes on BAS of zeolites has been widely reported.[36, 54] As proposed in Scheme 2 Route 2, the activated aromatic intermediates can react with the strong electronegativity of the chloride atom in BzCl molecule by releasing HCl simultaneously, which may affords a similar BzCl conversion with mesitylene over various Hβ zeolites with different BAS and LAS densities and strength (Table 4).

■ CONCLUSION

Hβ zeolites with different Si/Al ratios (10-30) have been prepared. ^{27}Al and ^{29}Si NMR revealed that Al atoms are well incorporated into the zeolite framework, introducing BAS on Hβ. ^{1}H MAS NMR spectroscopy was utilized to quantify the density of BAS, which decreased from 0.52 mmol/g to 0.41 mmol/g with increasing Si/Al ratio. ^{1}H MAS NMR studies using CD_3CN as

probe molecules demonstrated Hβ1 and Hβ2 exhibit a similar BAS strength, which is slightly lower than Hβ3 and Hβ4 at a higher Si/Al ratios.

Due to the shape selectivity, these Hβ zeolites are highly selective to desired DPM and substituted DPM products and avoided the generation of polyalkylated byproducts. They yielded a 100 % selectivity to DPM, BDB and BTB, while there is an 89.7 % to 92.1 % selectivity to 4-BMB, which was independent from acidic properties of H-Beta. Benzylation of different arenes over zeolite Hβ3 under the same conditions demonstrates the catalytic performance was in the order of xylene > toluene > benzene, in good consistent with the decrease of nucleophilicity and PA. A higher BzCl conversion of xylene than mesitylene has been attributed to its small molecular size and less structure hindrance.

It has been widely accepted the formation of benzyl cations ($C_6H_5CH_2^+$) on surface BAS is the initial step in the benzylation reactions, while LAS is inactive. Here, we found increasing the number of EFAl (acting as LAS) can strongly decrease the catalytic performance of Hβ zeolites, due to the strong adsorption of reactant/product molecules on these sites. In this work, we further revealed that more BAS with similar or higher strength on Hβ zeolites can contribute more aryl cation intermediates to react with benzyl chloride, and thus, promote the benzylation reactions (Scheme 2 route 2). Therefore, tailoring Hβ zeolites with less LAS and suitable BAS density is promising for the efficient production of DPM and substituted DPM products via benzylation reaction of arenes.

■ AUTHOR INFORMATION

Corresponding Author

*jun.huang@sydney.edu.au (Jun Huang); changhai@dlut.edu.cn (Changhai Liang)

Notes

The authors declare no competing financial interest

■ ACKNOWLEDGMENT

This work was supported by the Australian Research Council Discovery Projects (DP150103842), the Faculty's MCR Scheme, Energy and Materials Clusters and the Early Career Research Scheme and the Major Equipment Scheme from the University of Sydney.

■ REFERENCES

[1] Olah, G. A., *Friedel-Crafts Chemistry*. Wiley-Interscience: New York, **1973**.

[2] Chaube, V. D. Benzylation of Benzene to Diphenylmethane Using Zeolite Catalysts. *Catal. Commun.* **2004**, *5*, 321-326.

[3] Iovel, I.; Mertins, K.; Kischel, J.; Zapf, A.; Beller, M. An Efficient and General Iron-Catalyzed Arylation of Benzyl Alcohols and Benzyl Carboxylates. *Angew. Chem.-Int. Ed.* **2005**, *44*, 3913-3917.

[4] Olah, G. A.; Meyer, M. W. Friedel-Crafts Isomerization. 6. Aluminum Chloride-Catalyzed Isomerization of Fluorobiphenyls. *J. Org. Chem.* **1963**, *28*, 1912-1914

[5] Sun, Y. Y.; Walspurger, S.; Tessonnier, J. P.; Louis, B.; Sommer, J. Highly dispersed iron oxide nanoclusters supported on ordered mesoporous SBA-15: A very active catalyst for Friedel-Crafts alkylations. *Appl. Catal. A-Gen.* **2006**, *300*, 1-7.

[6] Pivsaart, S.; Okuro, K.; Miura, M.; Murata, S.; Nomura, M. Acylation of 2-methoxynaphthalene with acyl chlorides in the presence of a catalytic amount of Lewis-acids. *J Chem Soc Perk T 1* **1994**, 1703-1707.

[7] Serres, C.; Fields, E. K. Benzylation of arenes. *J. Am. Chem. Soc.* **1960**, *82*, 4685-4688.

[8] Bolton, A. P. *Zeolite chemistry and catalysis*. Am. Chem. Soc.: Washington DC, **1976**.

[9] Kirker-Othmer, *Encyclopedia of Chemical Technology*, 3rd Ed., **1978**, Vol. 2.

[10] Beltrame, P.; Zuretti, G.; Demartin, F. Benzylation of biphenyl with benzyl chloride over crystalline, amorphous, and MCM-41 solid acid catalysts. *Ind. & Eng. Chem. Res.* **2000**, *39*, 1209-1214.

[11] Choudhary, V. R.; Jana, S. K.; Kiran, B. P. Alkylation of benzene by benzyl chloride over H-ZSM-5 zeolite with its framework Al completely or partially substituted by Fe or Ga. *Catal. Lett.* **1999**, *59*, 217-219.

[12] Vinu, A.; Sawant, D. P.; Ariga, K.; Hartmann, M.; Halligudi, S. B. Benzylation of benzene and other aromatics by benzyl chloride over mesoporous AlSBA-15 catalysts. *Micro. Meso. Mater.* **2005**, *80*, 195-203.

[13] Coq, B.; Gourves, V.; Figueras, F. Benzylation of toluene by benzyl-chloride over protonic zeolites. *Appl. Catal. A-Gen.* **1993**, *100*, 69-75.

[14] Nandiwale, K. Y.; Thakur, P.; Bokade, V. V. Environmentally benign process for benzylation of toluene to mono-benzylated toluene over highly active and stable hierarchical zeolite catalyst. *Appl. Petro. Res.* **2015**, *5*, 113-119.

[15] Singh, A. P.; Jacob, B.; Sugunan, S. Liquid-phase selective benzylation of o-xylene using zeolite catalysts. *Appl. Catal. A-Gen.* **1998**, *174*, 51-60.

[16] Vinu, A.; Sawant, D. P.; Ariga, K.; Hossain, K. Z.; Halligudi, S. B.; Hartmann, M.; Nomura, M. Direct synthesis of well-ordered and unusually reactive FeSBA-15 mesoporous molecular sieves. *Chem. Mater.* **2005**, *17*, 5339-5345.

[17] Koyande, S. N.; Jaiswal, R. G.; Jayaram, R. V. Reaction kinetics of benzylation of benzene with benzyl chloride on sulfate-treated metal oxide catalysts. *Ind. & Eng. Chem. Res.* **1998**,

37, 908-913.

[18] Li, S.; Zhou, H.; Jin, C. H.; Feng, N. D.; Liu, F.; Deng, F.; Wang, J. Q.; Huang, W.; Xiao, L. P.; Fan, J. Formation of subnanometer Zr-WOx clusters within mesoporous W-Zr mixed oxides as strong solid acid catalysts for Friedel-Crafts alkylation. *J. Phys. Chem. C* **2014**, *118*, 6283-6290.

[19] Izumi, Y.; Ogawa, M.; Urabe, K. Alkali-metal salts and ammonium-salts of Keggin-type heteropolyacids as solid acid catalysts for liquid-phase Friedel-Crafts reactions. *Appl. Catal. A-Gen.* **1995**, *132*, 127-140.

[20] Salavati-Niasari, M.; Hasanalian, J.; Najafian, H. Alumina-Supported $FeCl_3$, $MnCl_2$, $CoCl_2$, $NiCl_2$, $CuCl_2$, and $ZnCl_2$ as Catalysts for the Benzylation of Benzene by Benzyl Chloride. *J. Mol. Catal. A-Chem.* **2004**, *209*, 209-214.

[21] Bachari, K.; Cherifi, O., Study of the benzylation of benzene and other aromatics by benzyl chloride over transition metal chloride supported mesoporous SBA-15 catalysts. *J. Mol. Catal. A-Chem.* **2006**, *260*, 19-23.

[22] Kamalakar, G.; Komura, K.; Kubota, Y.; Sugi, Y. Friedel-Crafts benzylation of aromatics with benzyl alcohols catalyzed by heteropoly acids supported on mesoporous silica. *J. Chem. Tech. Biot* **2006**, *81*, 981-988.

[23] Choudhary, V. R.; Jana, S. K.; Patil, N. S.; Bhargava, S. K. Friedel-Crafts type benzylation and benzoylation of aromatic compounds over H beta zeolite modified by oxides or chlorides of gallium and indium. *Micro. Meso. Mater.* **2003**, *57*, 21-35.

[24] Yu, Z.; Zheng, A.; Wang, Q.; Chen, L.; Xu, J.; Amoureux, J.-P.; Deng, F. Insights into the dealumination of zeolite HY revealed by sensitivity-enhanced Al-27 DQ-MAS NMR spectroscopy at high field. *Angew. Chem.-Int. Ed.* **2010**, *49*, 8657-8661.

[25] Jiang, Y.; Huang, J.; Dai, W.; Hunger, M. Solid-state nuclear magnetic resonance investigations of the nature, property, and activity of acid sites on solid catalysts. *Solid State Nucl. Magn. Reson.* **2011**, *39*, 116-141.

[26] Pfeifer, H.; Freude, D.; Hunger, M. Nuclear magnetic-resonance studies on the acidity of zeolites and related catalysts. *Zeolites* **1985**, *5*, 274-286.

[27] Diaz, E.; Ordonez, S.; Vega, A.; Auroux, A.; Coca, J. Benzylation of benzene over Fe-modified ZSM-5 zeolites: correlation between activity and adsorption properties. *Appl. Catal. A-Gen.* **2005**, *295*, 106-115.

[28] Bhatia, S. *Zeolite Catalysis: Principles and Applications*. CRC Press, Inc.,: Boca Raton, Florida, 1990.

[29] Treacy, M. M. J.; Newsam, J. M. 2 New 3-dimensional 12-Ring zeolite frameworks of which zeolite Beta is a disordered intergrowth. *Nature* **1988**, *332*, 249-251.

[30] Jacobs, P. A.; Mortier, W. J.; Uytterhoeven, J. B. Properties of zeolites in relation to their electronegativity-acidity, carboniogenic activity and strength of interaction in transition-metal complexes. *J. Inorg. & Nucl. Chem.* **1978**, *40*, 1919-1923.

[31] Mortier, W. J. Zeolite electronegativity related to physicochemical properties. *J. Catal.* **1978**, *55*, 138-145.

[32] Wang, Z.; Wang, L.; Jiang, Y.; Hunger, M.; Huang, J. Cooperativity of Brønsted and Lewis acid sites on zeolite for glycerol dehydration. *ACS Catal.* **2014**, *4*, 1144-1147.

[33] J. Stelzer, M. Paulus, M. Hunger, J. Weitkamp, Micro. Meso. Mater. 22 (1998) 1-8. Stelzer, J.; Paulus, M.; Hunger, M.; Weitkamp, J. Hydrophobic properties of all-silica zeolite Beta. *Micro. Meso. Mater.* **1998**, *22*, 1-8.

[34] Huang, J.; Jiang, Y.; Marthala, V. R. R.; Thomas, B.; Romanova, E.; Hunger, M.

Characterization and acidic properties of aluminum-exchanged zeolites X and Y. *J. Phys. Chem. C* **2008**, *112*, 3811-3818.

[35] Hunger, M.; Freude, D.; Pfeifer, H.; Prager, D.; Reschetilowski, W. Proton MAS NMR-studies of hydroxyl-groups in alkaline-earth cation-exchanged zeolite-Y. *Chem. Phys. Lett.* **1989**, *163*, 221-224.

[36] Huang, J.; Jiang, Y. J.; Marthala, V. R. R.; Wang, W.; Sulikowski, B.; Hunger, M. In Situ H-1 MAS NMR investigations of the H/D exchange of alkylaromatic hydrocarbons on zeolites H-Y, La,Na-Y, and H-ZSM-5. *Micro. Meso. Mater.* **2007**, *99*, 86-90.

[37] Deng, F.; Yue, Y.; Ye, C. H. Observation of nonframework Al species in zeolite Beta by solid-state NMR spectroscopy. *J. Phys. Chem. B* **1998**, *102*, 5252-5256.

[38] Jiao, J.; Kanellopoulos, J.; Wang, W.; Ray, S. S.; Foerster, H.; Freude, D.; Hunger, M. Characterization of framework and extra-framework aluminum species in non-hydrated zeolites Y by Al-27 spin-echo, high-speed MAS, and MQMAS NMR spectroscopy at B-0=9.4 to 17.6 T. *Phys. Chem. Chem. Phys.* **2005**, *7*, 3221-3226.

[39] Hunger, M.; Ernst, S.; Steuernagel, S.; Weitkamp, J. High-field H-1 MAS NMR investigations of acidic and non-acidic hydroxyl groups in zeolites H-Beta, H-ZSM-5, H-ZSM-58 and H-MCM-22. *Micro. Mater.* **1996**, *6*, 349-353.

[40] Beck, L. W.; Haw, J. F., Multinuclear NMR-studies reveal a complex acid function for zeolite-Beta. *J. Phys. Chem.* **1995**, *99*, 1076-1079.

[41] Lohse, U.; Parlitz, B.; Patzelova, V. Y Zeolite acidity dependence on the silicon/aluminum ratio. *J. Phys. Chem.* **1989**, 93, 3677-3683.

[42] Liu, C.; Li, G.; Hensen, E. J. M.; Pidko, E. A. Relationship between acidity and catalytic reactivity of faujasite zeolite: a periodic DFT study. *J. Catal.* **2016**, 344, 570-577.

[43] Li, S.; Zheng, A.; Su, Y.; Zhang, H.; Chen, L.; Yang, J.; Ye, C.; Deng, F. Brønsted/Lewis acid synergy in dealuminated HY zeolite: a combined solid-state nmr and theoretical calculation study. *J. Am. Chem. Soc.* **2007**, 129, 11161-11171.

[44] Gabrienko, A. A.; Danilova, I. G.; Arzumanov, S. S.; Toktarev, A. V.; Freude, D.; Stepanov, A. G. Strong acidity of silanol groups of zeolite Beta: evidence from the studies by IR spectroscopy of adsorbed CO and H-1 MAS NMR. *Microporous Mesoporous Mater.* **2010**, *131*, 210-216.

[45] Brunner, E.; Beck, K.; Koch, M.; Heeribout, L.; Karge, H. G. Verification and quantitative-determination of a new-type of Brønsted acid sites in H-ZSM-5 by H-1 Magic-Angle-Spinning Nuclear-Magnetic-Resonance Spectroscopy. *Microporous Mater.* **1995**, *3*, 395-399.

[46] Nakashima, S.; Takahashi, Y.; Kiguchi, M. Effect of the environment on the electrical conductance of the single benzene-1,4-diamine molecule junction. *Beilstein J. Nanotech.* **2011**, *2*, 755-759.

[47] Huang, J.; Jiang, Y.; Marthala, V. R. R.; Hunger, M. Insight into the mechanisms of the ethylbenzene disproportionation: transition state shape selectivity on zeolites. *J. Am. Chem. Soc.* **2008**, *130*, 12642-12644

[48] Choudhary, V. R.; Jana, S. K.; Narkhede, V. S. Benzylation and benzoylation of substituted benzenes over solid catalysts containing Ga- and Mg-oxides and/or chlorides derived from Ga-Mg-hydrotalcite by its HCl pre-treatment or calcination. *Appl. Catal. A-Gen.* **2002**, *235*, 207-215

[49] Cseri, T.; Bekassy, S.; Figueras, F.; Rizner, S. Benzylation of aromatics on ion-exchanged clays. *J. Mol. Catal. A-Chem.* **1995**, *98*, 101-107.

[50] Haw, J. F. Zeolite acid strength and reaction mechanisms in catalysist. *Phys. Chem. Chem. Phys.* **2002**, *4*, 5431-5441.

[51] Jenkins, S. J. Aromatic Adsorption on metals via first-principles density functional theory. *Proceedings of the Royal Soc. A-Mathematical Phys. and Eng. Sci.* **2009**, *465*, 2949-2976.

[52] Garbowski, E.; Primet, M. Adsorption of benzene on acidified alumina. *J. Chem. Soc.-Faraday Trans. I* **1987**, *83*, 1469-1476.

[53] Korman, C. S.; Lau, J. C.; Johnson, A. M.; Coleman, R. V. Studies of aromatic ring compounds adsorbed on alumina and magnesia using inelastic electron-tunneling. *Phys. Rev. B* **1979**, *19*, 994-1014.

[54] Beck, L. W.; Xu, T.; Nicholas, J. B.; Haw, J. F. Kinetic NMR and density-functional study of benzene H/D exchange in zeolites, the most simple aromatic-substitution. *J. Am. Chem. Soc.* **1995**, *117*, 11594-11595.